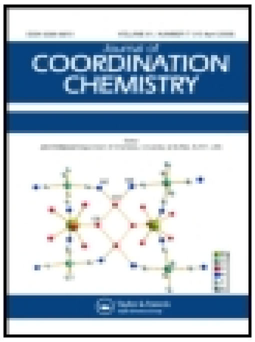

Taylor & Francis
Taylor & Francis Group

Journal of Coordination Chemistry

ISSN: 0095-8972 (Print) 1029-0389 (Online) Journal homepage: http://www.tandfonline.com/loi/gcoo20

Immobilized triazine bis[mercapto amine] complexes of Pd(0) anchored nickel ferrite as a nanocatalyst for C-C coupling reaction

Hossein Naeimi & Fatemeh Kiani

To cite this article: Hossein Naeimi & Fatemeh Kiani (2018): Immobilized triazine bis[mercapto amine] complexes of Pd(0) anchored nickel ferrite as a nanocatalyst for C-C coupling reaction, Journal of Coordination Chemistry, DOI: 10.1080/00958972.2018.1458229

To link to this article: https://doi.org/10.1080/00958972.2018.1458229

Publisher: Taylor & Francis
Journal: *Journal of Coordination Chemistry*

DOI: http://doi.org/10.1080/00958972.2018.1458229

Immobilized triazine bis[mercapto amine] complexes of Pd(0) anchored nickel ferrite as a nanocatalyst for C-C coupling reaction

HOSSEIN NAEIMI* and FATEMEH KIANI

Department of Organic Chemistry, Faculty of Chemistry, University of Kashan, Kashan, 87317-51167, I.R. Iran

Immobilized triazine bis[mercapto amine] complexes of Pd(0) ($NiFe_2O_4$@TABMA-Pd(0)) was easily synthesized and applied as highly efficient and versatile nanocatalyst for the synthesis of various *trans* stilbenes with high performance for the Heck coupling reaction of several types of aryl halides under thermal conditions. In short reaction time, excellent yields of *trans* stilbene derivatives have been achieved using $NiFe_2O_4$@TABMA-Pd(0) catalyst.

Keywords: $NiFe_2O_4$@TABMA-Pd(0), Styrene, Aryl halide, Heterogeneous catalyst, *Trans* stilbene derivatives

1. Introduction

One method for carbon–carbon bond forming is Heck coupling [1-3], which involves reaction between aryl halides and olefins in the presence of a base. Initially, aryl, benzyl, and vinyl halides are used as electrophiles, but many alkyl compounds are employed as the electrophiles [4]. Carbon–carbon bond formation by transition-metal catalyzed coupling reactions is a significant procedure in organic synthesis [5]. This method first reported in 1971 has become a powerful tool for various organic syntheses, preparation of advanced enantioselective natural products and pharmaceutically active ingredients, polymerization processes, production of pharmaceuticals, agrochemicals, advanced materials and fragrances [6-8]. Previously, phosphine ligands have been applied to stabilize active palladium intermediates, and great effects have been

---

*Corresponding author. Email: naeimi@kashanu.ac.ir

reported for Pd-catalyzed carbon-carbon coupling reactions. However, the oxygen and water sensitivity, expense, toxicity and lack of recoverability of these ligands prevents their use in a diversity of synthetic applications.

Mizoroki–Heck coupling reactions are usually catalyzed by soluble palladium complexes containing diverse ligands in water or organic solvents [9-13]. These homogeneous systems are the first option of chemists because of their high activity and selectivity; however, these are difficult to separate and reuse, often due to pollution with final products limiting their use in synthetic and industrial applications [14, 15]. To overcome these drawbacks, research on developing effective procedures for Pd complexes on several different solid supports, such as clays, [16] activated carbon, [17] microporous polymers, [18] and magnetic nanoparticles, have been performed.

Herein, we study a highly active catalytic system based on a Pd complex for Heck coupling reactions of styrene with various aryl halides using DMF as solvent.

2. Experimental

2.1. *General procedure for the synthesis of $NiFe_2O_4$@TABMA-Pd(0)*

Nickel ferrite nanoparticles ($NiFe_2O_4$) were synthesized by using co-precipitation according to the procedure reported [19]. The core-shell $NiFe_2O_4@SiO_2$ nanoparticles were obtained by a Stober method with minor modifications [20, 21]. The surface of silica nanoparticles can be easily functionalized through aminopropyltriethoxysilane according to the procedure reported [22]. For synthesis of ligand **3**, to a mixture of **1** (0.50 g) in dry toluene (30 mL) at 0 °C, 1,3,5-trichlorotriazine (TCT) (2 mmol, 0.37 g) and diisopropylethyl amine (2 mmol, 0.34 mL) were added and the mixture was stirred at 0 °C for 3 h. After consumption of TCT and production of **2**, cysteaminium chloride (4 mmol, 0.45 g) and diisopropylethyl amine (4 mmol, 0.68 mL) were slowly added to this mixture and refluxed in dry toluene for 24 h. The residue was separated from the mixture by an external magnet, washed with CH_2Cl_2 several times and dried at 80 °C to obtain **3**. The final catalyst nanoparticles were prepared as brown solids by addition of $Pd(OAc)_2$ (10 mg, 0.45 mmol) to a dispersed mixture of **3** in acetonitrile (5 mL) under nitrogen at room temperature. Then, the mixture was stirred for 6 h at 60 °C and an additional 45 min at 70 °C. The final complex was collected by an external magnet and washed repeatedly with ethanol to remove the unreacted $Pd(OAc)_2$, and then dried under air to obtain **4** (scheme 1). The 10 ml $NaBH_4$ solution (1 mmol) was added to the above solution with mechanical stirring at room temperature for 24 h. Then, the catalyst was separated from the mixture by centrifugation, washed several times with methanol to remove unreacted $Pd(OAc)_2$ and dried under vacuum to obtain a black solid powder.

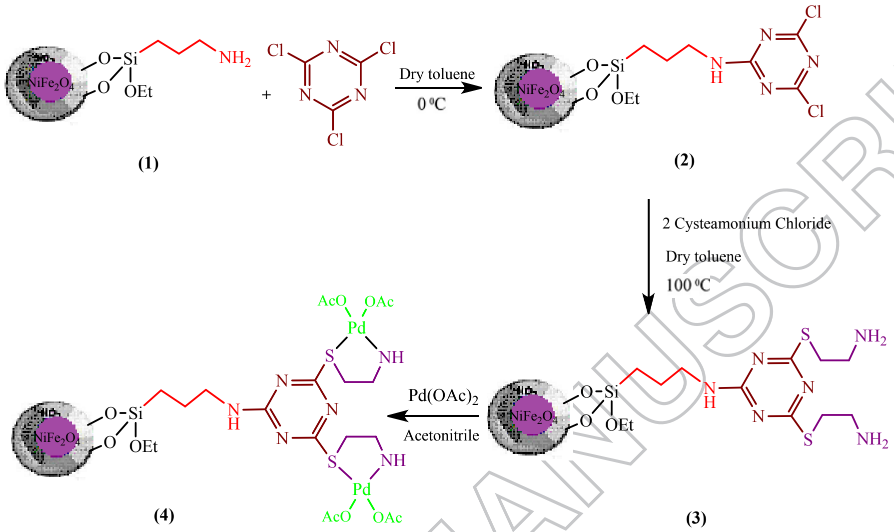

Scheme 1. Synthesis of the catalyst $NiFe_2O_4$@TABMA-Pd(0).

For synthesis of *trans*-stilbene derivatives, a mixture of selected aryl halide (1 mmol), styrene (1.2 mmol) and NEt_3 (2 mmol) in the presence of 0.015 g catalyst at 130 °C was reacted in DMF as solvent for 2.5-12 h according to table 1. The progress of the reaction was monitored by thin layer chromatography (n-hexane/ethyl acetate, 4:1). After completion of the reaction, the catalyst was separated by an external magnet, washed with absolute ethanol, dried, and used for the next reactions without further purification. After separation of the catalyst, ethyl acetate (15 mL) was added and the organic phase was washed with water (3 × 10 mL), and dried over anhydrous $MgSO_4$. The resulting solution was evaporated under vacuum to give the crude product. Column chromatography of the crude product on silica gel using n-hexane or different mixtures of n-hexane, ethyl acetate as the eluents afforded the highly pure product.

3. Results and discussion

The method for preparation of the catalyst is shown in scheme 1. In order to characterize the catalyst structure, the synthesized nano catalyst was analyzed using Fourier transform infrared

(FT-IR) spectra, scanning electron microscopy (SEM), energy-dispersive X-ray spectroscopy (EDX), vibrating sample magnetometer (VSM), and also, thermo-gravimetric analysis (TGA) techniques.

Figure 1 shows the FT-IR spectrum of $NiFe_2O_4$ NPs, $NiFe_2O_4@SiO_2$, $NiFe_2O_4@SiO_2–NH_2$ NPs and $NiFe_2O_4$@TABMA from 400–4000 cm^{-1}. The spectrum presents characteristic bands at 3415, 2920, 1620, 597 and 421 cm^{-1}. Bands at 3415 and 1620 cm^{-1} can be assigned to the stretching modes of absorbed water. The band at 597 cm^{-1} is attributed to Fe—O vibration. The band at 421 cm^{-1} can be assigned to Ni—O vibrations. In all three spectra, the peaks of $NiFe_2O_4$ were observed at 421–601 $cm^{−1}$, which could be attributed to the absorption of Fe—O and Ni—O bonds. In $NiFe_2O_4@SiO_2$, $NiFe_2O_4@SiO_2–NH_2$, and final catalyst spectra the intense peaks at 1091, 1095 and 1096 $cm^{−1}$ were derived from the Si–O–Si stretching vibrations. These peaks proved that SiO_2 has coated the surface of $NiFe_2O_4$. In the $NiFe_2O_4@SiO_2–NH_2$ spectrum, the peaks at 1635 and 1540 $cm^{−1}$ could be attributed to the C–N stretch and NH_2 bending vibration. The peak at 2945 $cm^{−1}$ is related to the CH_2 stretch, the peak at 1466 $cm^{−1}$ is related to bending vibration of CH_2 and the peak at 3439 $cm^{−1}$ is assigned to the N–H stretch. These peaks confirmed that $NiFe_2O_4@SiO_2–NH_2$ NPs are prepared. The FT-IR spectrum of $NiFe_2O_4$@TABMA showed absorption bands at 1625 $cm^{−1}$ (C=N), 2983 $cm^{−1}$ (C–H), 3421 $cm^{−1}$ (N–H stretching vibration) and 778 $cm^{−1}$ (C–S stretching vibration).

Figure 2 shows the SEM image of $NiFe_2O_4$ and $NiFe_2O_4$@TABMA-Pd(0); spherical morphology with an average diameter of 25-35 nm for $NiFe_2O_4$ and 40 nm for $NiFe_2O_4$@TABMA-Pd(0) was observed. Also, the elemental analysis for catalyst was performed. Figure 3 shows the EDX spectra of $NiFe_2O_4$@TABMA-Pd(0). The results showed the presence of C (26.7), N (15.98), O (33.43), Si (3.68), S (4.80), Fe (6.17) and Pd (7.59) in the composites which confirm that the catalyst has been synthesized.

The loading of Pd in $NiFe_2O_4$@TABMA-Pd(0) was determined using inductively coupled plasma atomic emission spectroscopy (ICP-AES) and was 4.93 wt% (0.27 mmol g^{-1}).

Thermal stability of the catalyst was investigated by TGA and the related curves are demonstrated in figure S1 (Supporting Information). Herein TGA analysis curves of $NiFe_2O_4@SiO_2$ and $NiFe_2O_4$@TABMA-Pd(0) are compared. Both curves have similar characteristics. As demonstrated in figure 4a, 6% decrease in weight before 150 °C is attributed to removal of surface hydroxyl groups and physically adsorbed solvent and water molecules trapped in the SiO_2 layer. The weight loss of 7% between 400 and 600 °C is attributed to decomposition of less stable functional groups, for example hydroxyl grafted to the silica surface. As illustrated in figure 4b, small weight loss (10%) between 150 °C and 250 °C is attributed to the trapped water. The organic components (40%) were lost between 250 and 400 °C. These results show the catalyst is stable up to 250 °C and can be used in organic synthesis.

Magnetic properties of $NiFe_2O_4$ nanoparticles and $NiFe_2O_4$@TABMA-Pd(0) were investigated with VSM at room temperature (figure S2 (Supporting Information)). Magnetization of samples could be completely saturated at fields up to 1.0 T and the saturation magnetization of samples decreased from 35 to 7 emug^{-1} because of the functionalization by extra organic layer. Furthermore, these results illustrate that the magnetization decreases by coating and functionalization. It is important that a catalyst possess enough magnetic properties for its experimental application.

To examine the catalytic performance of the nanocatalyst and to characterize optimal conditions for Mizoroki–Heck coupling reaction, iodobenzene and styrene were selected as model reagents and were investigated under different parameters such as solvent, various amounts of catalyst and the effect of different temperatures.

In our first set of experiments, we examined efficiency of the different solvents in the model reaction. Several organic solvents, acetonitrile, ethanol, dimethylformamide, dimethyl sulfoxide and toluene, were examined. According to data in table 1, entry 4, DMF was the most efficient solvent for this transformation. Other solvents gave only moderate yields of the product.

In continuation of this research, the activity of the catalyst in different amounts on the reaction was investigated. No reaction was observed in the absence of catalyst at 140 °C (table 1, entry 6). The results demonstrated that on heating and 0.015 g of the $NiFe_2O_4$@TABMA-Pd(0) catalyst, the reaction time is decreased to 2.5 h and the yield increased sharply to 96% (table 1, entry 9). The reaction temperature was also optimized. The model reaction was performed in the presence of 0.015 g of $NiFe_2O_4$@TABMA-Pd(0) catalyst in DMF under various temperatures to investigate the best operating suitable temperature. The best temperature was 130 °C (table 1, entry 11).

In the next step, to obtain a suitable base for the coupling reaction, different bases were studied in this reaction. Among the various bases screened, NEt_3 was found to be the best base for this reaction (table 2, entry 4). Bases such as Na_2CO_3 and K_2CO_3 gave moderate yields of the product.

Furthermore, the kinetic effects of $NiFe_2O_4$@TABMA-Pd(0) on Heck cross-coupling reaction of iodobenzene and styrene were investigated. The results are shown in figure 4. As can be seen in figure 4, the reaction efficiency is higher and the reaction proceeds at a higher rate at the initial times than the end times.

After optimization of the reaction conditions, a broad range of structurally diverse aryl halides were reacted with styrene in the presence of 0.015 g of $NiFe_2O_4$@TABMA-Pd(0) catalyst and 2 mmol NEt_3 with DMF as solvent at 130 °C and the results are displayed in table 3. As shown in table 3, the reaction performed efficiently in high yield between 2.5-12 h at 130 °C. Also, in the presence of Pd nanocatalyst, excellent product yields were achieved in shorter reaction time.

In order to show the merit of this proposed research, we compared the obtained results with recently reported results [32-36]. For this purpose, the reactions of iodobenzene and styrene using Pd complex in DMF at 130 °C in the presence of 2 mmol of NEt_3 were chosen as a model reaction and the comparison was performed on the basis of reaction time and obtained yields (table 4, entry 5 *vs.* entries 1-4). The properties which make our research better than previous procedures are mild reaction conditions, environmentally benign, simple recycle of the nano catalyst by an external magnet, reusability of the catalyst for six times without considerable loss of catalytic activity, excellent yields of *trans* stilbene and very short reaction times.

The recyclability of the catalyst was investigated in the coupling of iodobenzene. After completion of the reaction, the catalytic system was separated from the reaction mixture using an external magnet and the residual catalyst was washed, dried and reused in subsequent reactions. After six cycles (figure 5), the catalyst had approximately the same activity and corresponding product in high yields.

4. Conclusion

Here we have used $NiFe_2O_4$@TABMA-Pd(0) as a highly active heterogeneous catalyst in the Heck coupling reactions. This reaction produced the corresponding *trans*-coupled products stereoselectively in high yields and acceptable reaction times. The catalyst can be separated by an external magnet and reused several times without significant loss of activity, which is an additional sustainable characteristic of this method.

Acknowledgments

The authors are grateful to University of Kashan for supporting this work by Grant No. 159148/72.

References

[1] A.V. Martínez, A. Leal-Duaso, J.I. García, J.A. Mayoral. *RSC Adv.*, **5**, 59983 (2015).

[2] V.P. Petrović, S. Marković, Z.D. Petrović. *Monatsh. Chem.*, **143**, 1497 (2012).

[3] M. Nasrollahzadeh, S.M. Sajadi, E. Honarmand, M. Maham. *New J. Chem.*, **39**, 4745 (2015).

[4] S.-S. Wang, G.-Y. Yang. *Catal. Sci. Technol.*, **6**, 2862 (2016).

[5] C.-S. Guo, Y.-H. Du, Z.-Z. Huang. *Chem. Commun.*, **47**, 3995 (2011).

[6] K. Sakoda, J. Mihara, J. Ichikawa. *Chem. Commun.*, 4684 (2005).

[7] L.A. Arnold, W. Luo, R.K. Guy. *Org. Lett.*, **6**, 3005 (2004).

[8] A.B. Dounay, L.E. Overman, A.D. Wrobleski. *J. Am. Chem. Soc.*, **127**, 10186 (2005).

[9] K.H. Ahn, D.J. Yoo, J.S. Kim. *Tetrahedron Lett.*, **33**, 6661 (1992).

[10] H.G. Richey Jr., J. Farkas Jr. *J. Org. Chem.*, **52**, 479 (1987).

[11] Z. Regaïnia, M. Abdaoui, N.-E. Aouf, G. Dewynter, J.L. Montero. *Tetrahedron*, **56**, 381 (2000).

[12] T. Mizoroki, K. Mori, A. Ozaki. *Bull. Chem. Soc. Jpn.*, **44**, 581 (1971).

[13] R.F. Heck. *Acc. Chem. Res.*, **12**, 146 (1979).

[14] Q.L. Luo, J.-P. Tan, Z.F. Li, Y. Qin, L. Ma, D.R. Xiao. *Dalton Trans.*, **40**, 3601 (2011).

[15] L.S. Søbjerg, D. Gauthier, A.T. Lindhardt, M. Bunge, K. Finster, R.L. Meyer, T. Skrydstrup. *Green Chem.*, **11**, 2041 (2009).

[16] A.F. Littke, G.C. Fu. *J. Am. Chem. Soc.*, **123**, 6989 (2001).

[17] M. Seki. *Synthesis*, **2006**, 2975 (2006).

[18] H. Lim, M.C. Cha, J.Y. Chang. *Polym. Chem.*, **3**, 868 (2012).

[19] K. Maaz, S. Karim, A. Mumtaz, S. Hasanain, J. Liu, J. Duan. *J. Magn. Magn. Mater.*, **321**, 1838 (2009).

[20] L. He, Z. Li, J. Fu, Y. Deng, N. He, Z. Wang, H. Wang, Z. Shi, Z. Wang. *J. Biomed. Nanotechnol.*, **5**, 596 (2009).

[21] Z. Li, L. He, Z. Shi, H. Wang, S. Li, H. Liu, Z. Wang, N. He. *J. Biomed. Nanotechnol.*, **5**, 505 (2009).

[22] H. Jiang, X. Zeng, Z. Xi, M. Liu, C. Li, Z. Li, L. Jin, Z. Wang, Y. Deng, N. He. *J. Biomed. Nanotechnol.*, **9**, 674 (2013).

[23] X. Cui, Z. Li, C. Z. Tao, Y. Xu, J. Li, L. Liu, Q.X. Guo. *Org. Lett.*, **8**, 2467 (2006).

[24] G. Ren, X. Cui, E. Yang, F. Yang, Y. Wu. *Tetrahedron*, **66**, 4022 (2010).

[25] B.R. Baker, R.E. Gibson. *J. Med. Chem.*, **14**, 315 (1971).

[26] Y.G. Zhang, X.L. Liu, Z.Y. He, X.M. Li, H.J. Kang, S.K. Tian. *Chem. Eur. J.*, **20**, 2765 (2014).

[27] M. Gozin, A. Weisman, Y. Ben-David, D. Milstein. *Nature*, **364**, 699 (1993).

[28] K.V. Kutonova, M.E. Trusova, A.V. Stankevich, P.S. Postnikov, V.D. Filimonov, Beilstein. *J. Org. Chem.*, **11**, 358 (2015).

[29] L.R. Moore, E.C. Western, R. Craciun, J.M. Spruell, D.A. Dixon, K.P. O'Halloran, K.H. Shaughnessy. *Organometallics*, **27**, 576 (2008).

[30] R. Bandari, T. Höche, A. Prager, K. Dirnberger, M.R. Buchmeiser. *Chem. Eur. J.*, **16**, 4650 (2010).

[31] A. Chaieb, A. Khoukh, R. Brown, J. François, C. Dagron-Lartigau. *Opt. Mater.*, **30**, 318 (2007).

[32] R.N. Baig, R.S. Varma. *Chem. Commun.*, **49**, 752 (2013).

[33] B. Baruwati, D. Guin, S.V. Manorama. *Org. Lett.*, **9**, 5377 (2007).

[34] R. Heck, J. Nolley Jr. *J. Org. Chem.*, **37**, 2320 (1972).

[35] C.S. Consorti, M.L. Zanini, S. Leal, G. Ebeling, J. Dupont. *Org. Lett.*, **5**, 983 (2003).

[36] A.S. Gruber, D. Pozebon, A.L. Monteiro, J. Dupont. *Tetrahedron Lett.*, **42**, 7345 (2001).

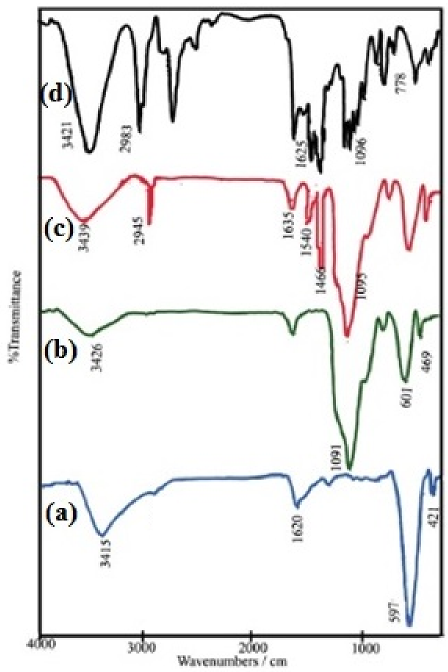

Figure 1. FT-IR spectrum of a) $NiFe_2O_4$ NPs, b) $NiFe_2O_4@SiO_2$, c) $NiFe_2O_4@SiO_2–NH_2$ NPs and d) $NiFe_2O_4$@TABMA.

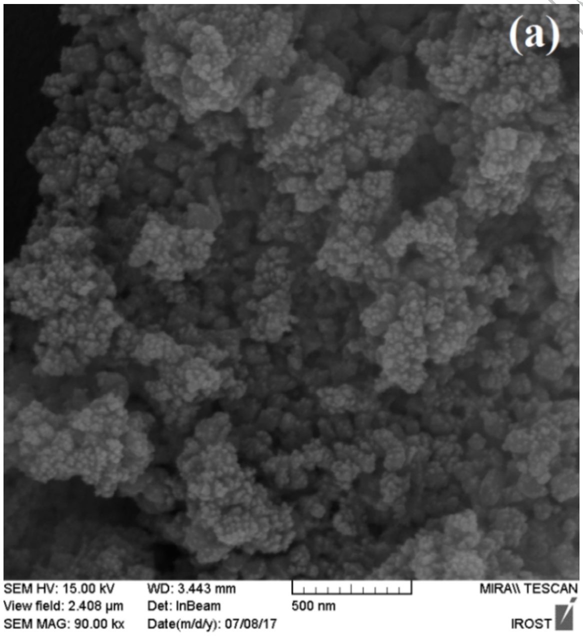

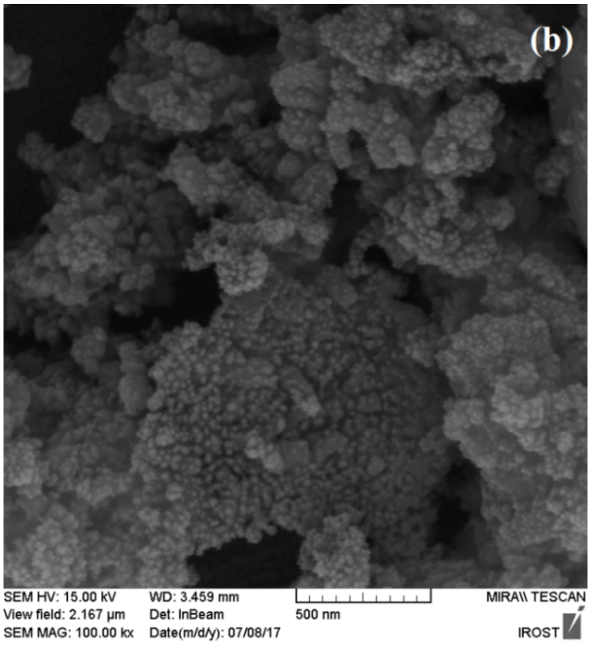

Figure 2. SEM images of $NiFe_2O_4$ nanoparticles (a) $NiFe_2O_4$@TABMA-Pd(0) (b).

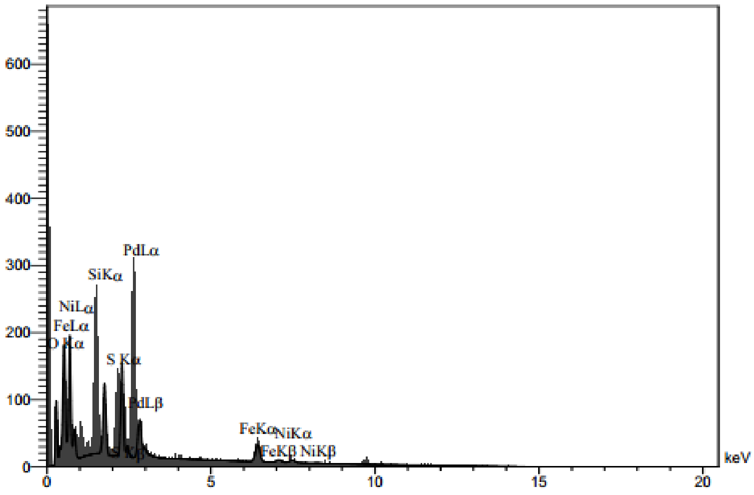

Figure 3. EDX spectrum of the $NiFe_2O_4$@TABMA-Pd(0).

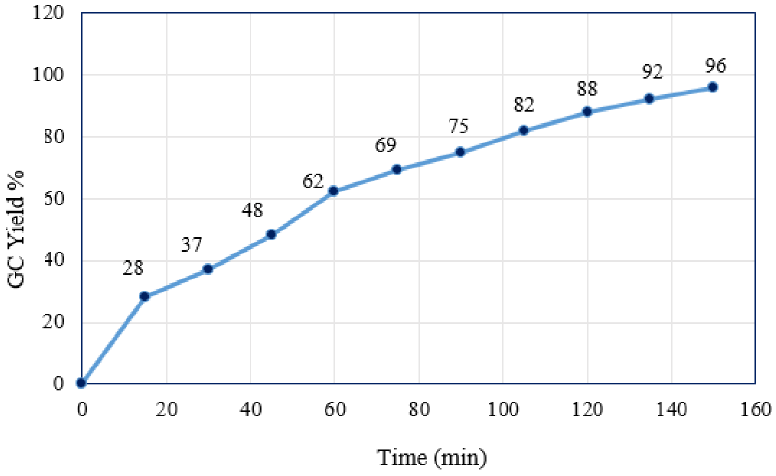

Figure 4. Kinetic effect diagram of $NiFe_2O_4$@TABMA-Pd(0) on the reaction.

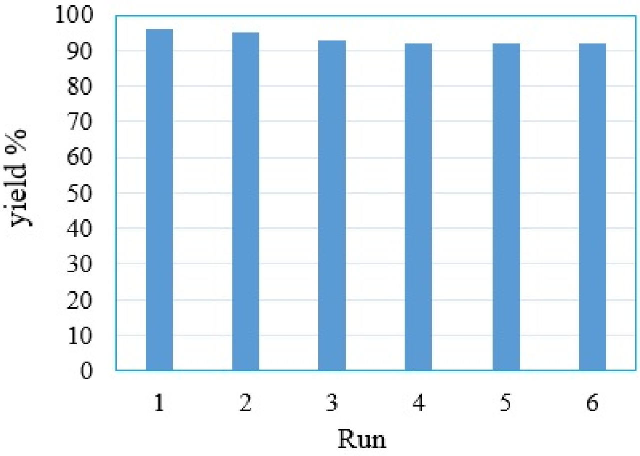

Figure 5. Reusability of catalyst for the synthesis of *trans* stilbene.

Table 1. Optimization of the various amounts of catalyst, temperature and solvent[a].

Entry	Cat. (g)	T (°C)	Solvent	Time (h)	Yield (%)
1	0.020	140	EtOH	3.5	83
2	0.020	140	CH_3CN	4.5	75
3	0.020	140	DMSO	4	79
4	0.020	140	DMF	2.5	96
5	0.020	140	Toluene	5	49
6	0	140	DMF	15	0
7	0.005	140	DMF	4	61
8	0.010	140	DMF	3.5	78
9	0.015	140	DMF	2.5	96
10	0.020	140	DMF	2.5	96
11	0.015	130	DMF	2.5	96
12	0.015	120	DMF	3	92
13	0.015	110	DMF	4.5	87

[a] Reaction conditions: iodobenzene (1 mmol), styrene (1.2 mmol) and NEt_3 (2 mmol) in solvent.

Table 2. Optimization of the different bases in reaction[a].

Entry	Base	Base amount (mmol)	Yield[b]
1	KOH	2	55
2	$NaHCO_3$	2	46
3	K_3PO_4	2	78
4	NEt_3	2	96
5	$NaHCO_3$	2	57
6	NEt_3	2.5	96
7	NEt_3	1.5	90

[a] Reaction conditions: iodobenzene (1 mmol), styrene (1.2 mmol), 130 °C, in DMF as solvent (5 mL). [b] Isolated yield.

Table 3. Mizoroki–Heck cross-coupling of coupling of aryl halides and styrene in the presence of $NiFe_2O_4$@TABMA-Pd(0)[a].

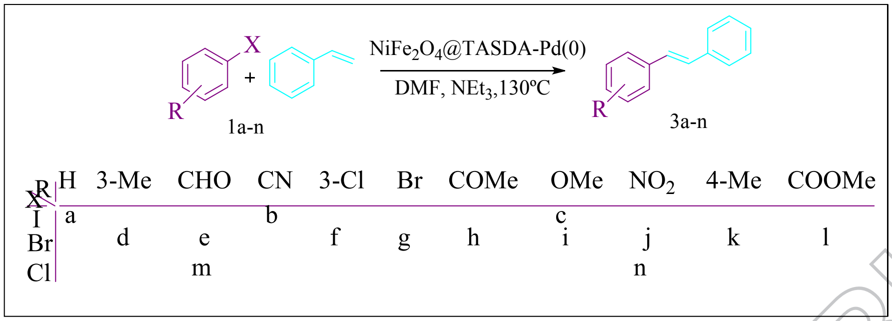

X \ R	H	3-Me	CHO	CN	3-Cl	Br	COMe	OMe	NO$_2$	4-Me	COOMe
I	a			b				c			
Br		d	e		f	g	h	i	j	k	l
Cl			m						n		

Entry	Aryl halide	Product	Thermal conditions[b] Time (h)/Yield[c] (%)	Ref.
1	1a	3a	2.5/96	[23]
2	1k	3k	5.5/87	[24]
3	1e	3e	6/90	[25]
4	1d	3d	5/81	[26]
5	1f	3f	7/87	[25]
6	1c	3c	3/78	[27]
7	1l	3l	7/80	[28]
8	1h	3h	7/94	[29]
9	1j	3j	6/94	[30]
10	1b	3b	2.5/98	[24]
11	1g	3g	7/90	[31]
12	1n	3n	11/66	[30]
13	1i	3i	9/83	[27]
14	1m	3m	12/65	[25]

[a] Reaction conditions: iodobenzene (1 mmol), styrene (1.2 mmol) and NEt_3 (2 mmol) in solvent. [b] at 130 °C. [c] Isolated yield.

Table 4. Comparison of the results in this research with various reports in the literature.

Entry	Catalyst	Time (h)	Yield (%)[a]	Ref.
1	Pd/MFC	2	66	[33]
2	Palladium acetate	2	75	[34]
3	Chloropalladated	48	68	[35]
4	$PdCl_2(SEt_2)_2$	23	71	[36]
5	$NiFe_2O_4$@TABMA-Pd(0)	2.5	96	This work

[a] Isolated yield.

Graphical abstract: